Hygrothermal assessment of internally insulated solid masonry walls fitted with exterior hydrophobization and deliberate thermal bridge

Jensen, Nickolaj Feldt; Bjarløv, Søren Peter; Rode, Carsten; Odgaard, Tommy Riviere

Published in:
Ce/papers

Link to article, DOI:
10.1002/cepa.868

Publication date:
2018

Document Version
Peer reviewed version

Nickolaj Feldt Jensen (corresponding author)
Søren Peter Bjarløv (co-author 1)
Carsten Rode (co-author 2)
Tommy Riviere Odgaard (co-author 3)

Hygrothermal assessment of internally insulated solid masonry walls

Fitted with exterior hydrophobization and deliberate thermal bridge

Relative humidity (RH) and temperature were measured in several solid masonry walls with embedded wooden beams, fitted with AAC thermal insulation on the interior surface and exposed to a cool, temperate climate. The field study was based on the use of a 40-feet insulated reefer container reconfigured with 8 1x2 m holes containing the solid masonry walls. The study investigated the influence of AAC thermal insulation on the interior side with a combination of exterior hydrophobization and a deliberate thermal bridge in front of the embedded wooden wall plate using a material with higher thermal conductivity. Validated HAM simulations were used to investigate the effect of controlling the indoor humidity, and how this would affect the theoretical risk predictions from the damage models. Experimental findings indicate that hydrophobization of solid masonry walls with internal insulation have both positive and negative effects on the moisture balance of the wall, in relation to moisture induced damage, and that a deliberate thermal bridge installed in front of the embedded wooden wall plate can reduce the moisture content in the wooden elements. Simulation findings indicate that a combination of exterior hydrophobization and decreased indoor moisture load can reduce the RH to acceptable levels in relation to moisture induced damage at the interface between existing wall and new insulation. No major changes were observed in relation to the risk of frost damage at the exterior surface.

Keywords: internal insulation; hydrophobization; damage models; mineral insulation board; field study.

1 Introduction

With an increasing desire towards reduction of the global energy demand and the carbon foot-print, an increased focus has been put on the building sector. Granted that the exiting building stock consists of a large share of buildings constructed prior to 1945, yielding a great potential towards reaching these goals as documented in the segment study by Odgaard et al. (1); many of which were built with solid masonry exterior walls. A large portion of these buildings are considered as worthy of preservation, posing several challenges with respect to renovation of the exterior walls as major exterior alterations often are prohibited. This often leaves internal post insulation as the only option. Previous research has shown sizable energy saving potential for internal insulation of solid masonry walls (2) (3) (4) (5); however, from a building physics point of view internal insulation is considered as problematic since the insulation reduces the heat flow to the exiting wall, which as a result becomes colder (6) (7) (8) (9). This results in an increased risk of condensation in the existing wall. Findings from recent experimental (2) and simulation (3) (4) (6) studies investigating the performance of solid masonry walls fitted with traditional and new internal insulation systems have shown worse hygrothermal conditions and increased risk of moisture induced damages. The aim of the research project is to find robust solutions to counteract this phenomenon.

The present paper presents a field study and a simulation study of internally insulated solid masonry walls located in a cool temperate climate. The insulation system studied is diffusion-open, capillary active and based on light-weight autoclaved aerated concrete (AAC). Temperature and RH were measured during the experimental period in eight test walls with different parameter variations. The measured data was later used for modelling and validation of the simulation models. Subsequently an assessment of the hygrothermal conditions in the test walls and simulation models was carried out using damage models for mould growth, wood decay and frost damage.

The research project tested the insulation system in combination with exterior hydrophobization and a deliberate thermal bridge; to investigate the hygrothermal performance in the masonry walls and in the embedded wooden wall plate and beam end, when the heat flow was increased locally around these elements.

2 Methods

The test walls were constructed to resemble Danish historic multi storey buildings from the period 1850-1930, both in relation to design and materials. In the following the experimental setup and the simulation models are described in detail.

2.1 Experimental setup

The experimental setup was comprised of a 40-foot insulated reefer container, into which eight 1 x 2 m cut-outs were made in the façade. Next, eight identical test walls with the dimensions (HxWxD) 1987 mm by 948 mm by 358 mm (1½ stones thick with 10 mm internal rendering) were constructed in cut-outs (Figure 1). Each test wall was constructed as a 3-dimensional set-up with a wooden floor construction and a ½-stone internal masonry wall with render on both sides (Figure 2). The adjacent elements were included in the study to replicate potential problems at the joints due to thermal bridges. The wooden floor construction consisted of a 100 x 100 mm wood wall plate embedded into the masonry wall, supporting a 175 x 175 mm wooden beam end embedded 100 mm. The floor construction was closed off using 15 mm oriented strand board (OSB), and to replicate the traditional clay pugging layers between the beams 100 mm of mineral wool was used. To best replicate the hygrothermal conditions occurring in the historic buildings, the test walls were constructed using yellow soft-moulded masonry brick and 7.7% air hardened lime mortar with a grain size of 0-4 mm; resembling the traditional masonry bricks and lime mortar used in buildings from the period 1850 to 1930. The lime mortar was used for the mortar joints and internal render. During the construction of the test walls, special attention was put on reducing potential sources of error like unintentional transport of heat, air and moisture. This was achieved through several measures including: 1) Hygric and thermal decoupling around the test walls with mineral wool insulation and vapour retarder. 2) Sealing of joints using mastic sealant. 3) Rain water run-off through flashings and roof construction with gutters. 4) Raising the container to prevent water splashing up.

The experiment was conducted at the test site of the Department of Civil Engineering at the Technical University of Denmark (DTU), in Kongens Lyngby, Denmark (55.79°N, 12.53°E).

Figure 1 a) External view of the reefer container and the test walls. b) Photos from the construction process. Source: Søren Peter Bjarløv

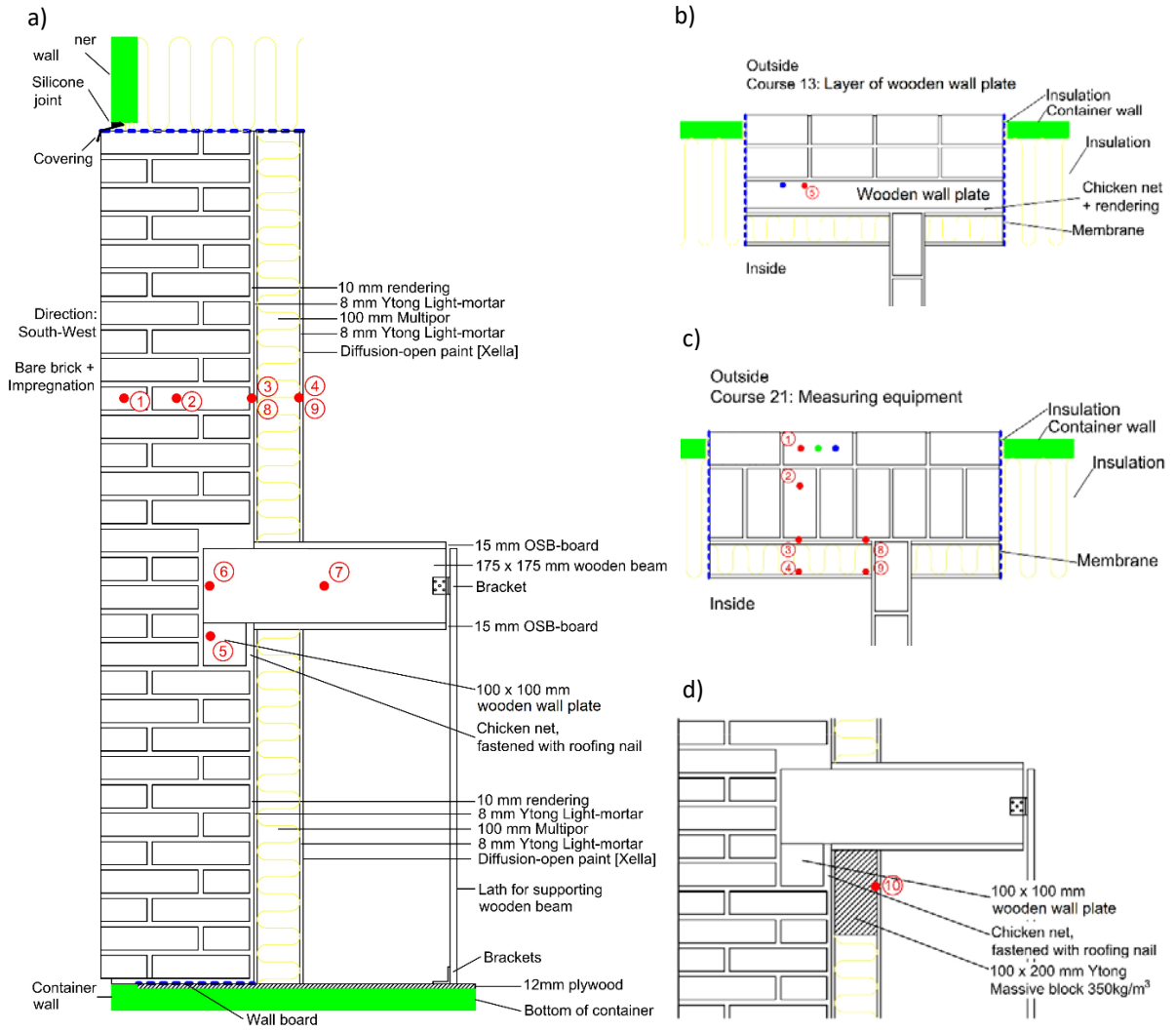

Figure 2 Sensor points: a) Vertical section of a test wall. b) Horizontal section through the 13th brick course. c) Horizontal section through the 21th brick course. d) Vertical section through the deliberate thermal bridge. Source: Tommy Riviere Odgaard

2.1.1 Variations

Each of the eight test walls in the experimental setup was an element in a set of parameter variations representing different scenarios. In this paper, four of the test walls are presented: Wall 5) Uninsulated, un-hydrophobized reference wall. Wall 2) Un-hydrophobized wall with internal insulation. Wall 3) Wall with internal insulation and exterior hydrophobization. Wall 6) Wall with internal insulation, exterior hydrophobization, and deliberate thermal bridge.

The internal insulation system was comprised of 8 mm light-mortar, 100 mm AAC insulation board, 8 mm Light-mortar, and diffusion-open paint on the interior surface. The hydrophobization was comprised of a silane/siloxane-based cream with 40% active ingredient. The deliberate thermal bridge was comprised of a 100 by 200 mm AAC block, with a density of 350 kg/m^3, installed in front of the embedded wooden wall plate, see Figure 2d. The purpose of the deliberate thermal bridge was to provide higher temperatures in the wooden wall plate and beam end, to possibly reduce the risk of moisture induced damages. Note that the insulation system and the hydrophobization were installed according to the manufacturer's recommendations, by people dispatched by the respective companies.

2.1.2 Measurement equipment

Temperature and RH were logged every 10 minutes during the experimental period using digital HYT221 sensors. Each test wall was fitted with nine sensors (Figure 2a-c), except for wall 6 which had a 10th sensor installed in the deliberate thermal bridge (Figure 2d). Two sets of sensors were installed inside the container, and one sensor set outside, behind a cladding board. Sensor accuracy was for RH ±1.8% at 23°C, between 0% and 90% RH, and for temperature ±0.2K between 0°C and 60°C. The sensors had a measurement range of 0% to 100% RH, and temperatures from −40°C to 125°C. Prior to installation, the sensors were calibrated using saturated salt solutions, and the calibration equations were applied before assessment. Data was logged from May 1, 2015. In addition, weather data was obtained from DTU's weather station, located on a nearby building 200 m west-southwest of the test site.

2.1.3 Boundary conditions

The test walls were oriented towards southwest (compass angle of 237°), which in Denmark is the prevailing wind direction and is thus treated as the most critical orientation for wind driven rain (WDR). Furthermore, WDR in combination with high solar radiation from south pose a potential risk for moisture transport through the wall towards the indoor environment.

The container was conditioned to 20 °C and 60% RH, corresponding to the upper limit of indoor climate class 3 (10). Dehumidification or cooling was not used. Thus, fluctuations could occur. Furthermore, the container was fitted with two fresh air dampers, providing air change rate of ca. 0.5 h^{-1}, which is common in Danish residential buildings (11).

2.2 Simulation study

1-D simulations were carried out in the software Delphin, to investigate the hygrothermal performance of an internally insulated solid masonry wall with and without exterior hydrophobization in combination with reduced indoor RH, for example by mechanical ventilation.

2.2.1 Model composition

Simulation models for Wall 2 (Un-hydrophobized with internal insulation) and Wall 3 (Hydrophobized with internal insulation) were modelled and validated using measured data (sensor 1-4, external and internal climates) by (12), and were further developed for this project. Furthermore, material data for the individual layers were obtained from the Delphin database, except for the historic brick which was obtained from a previous DTU project (13). To simulate the hydrophobization of Wall 3, the water uptake coefficient, A_w, was reduced by a factor 1000 for the outermost 10 mm of the masonry. Material properties used in Delphin are shown in Table 1. In the validation process material parameters and boundary conditions were adjusted down/up by maximum 10%.

Table 1 Material properties

Material	Density [kg/m^3]	λ_{Dry} [W/(m^2·K)]	μ [-]	A_w [kg/(m^2·s$^{0.5}$)]
Masonry brick	1713	0.518	11.56	0.313
Hydrophobized masonry brick	1713	0.518	11.56	0.000313
Historic lime plaster	1800	0.82	12	0.127
Multipor mineral insulation board	98.5	0.044	3	0.006
Glue mortar for mineral insulation	830	0.155	13	0.0031

2.2.2 Boundary conditions

The wall models were simulated for four years, where a two-year initial simulation period was used to reach a quasi-steady state before the measured data was introduced, as recommended by (14). For the initial simulation period, Design Reference Year (DRY) climate data for Copenhagen was used. The DRY data set did not include rain load, this was obtained from DTU's weather station, along with wind, rain and short-wave radiation during the measurement period. For long-wave radiation, DTU DRY data was used. For the indoor conditions, two scenarios were simulated: 1) Using measured data, with a setpoint of 60% RH, and 2) RH fixed to 40%, based on the normal RH range during winter of 30 to 50% in residential buildings (8).

Coefficients for the boundary conditions in Delphin:

- Rain exposure coefficient 0.6 [-]
- Solar reflection coefficient of the surrounding ground (albedo) 0.2 [-]
- Solar absorption coefficient of the building surface 0.7 [-]
- Longwave emission coefficient of the building surface 0.9 [-]
- Surface heat transfer coefficient, External/Internal 25 / 4 [W/(m^2·K)]
- Surface moisture transfer coefficient, External/Internal 2e-7 / 3e-8 [s/m]

Lastly, like the experimental setup, the simulated walls were oriented towards southwest.

2.3 Damage models

Several damage models were used in the project to assess the hygrothermal conditions of the test walls and simulation models over time, to produce a theoretical prediction of the risk of mould growth, wood decay and frost damage. Widely used damage models were chosen for the assessment.

2.3.1 Mould growth

The risk of mould growth was determined using the mathematical model by Hukka and Viitanen (the "VTT model") (15) (16) (17). The model calculates the critical RH as a function of temperature, and growth occurs if $RH \geq RH_{crit}$ and T > 0 °C. Output from the model is the mould index (M), ranging from 0 to 6, where 0 corresponds no growth and 6 to heavy tight growth. The mould modelling was carried out using the material class "medium resistant" and a decline factor of "relatively low"; corresponding to concrete products. Mould modelling was performed for the interior surface, and at the interface between masonry and insulation.

2.3.2 Wood decay

The risk was determined using the mathematical model for wood decay by Viitanen et. al. (18). The decay model consists of two processes: 1) Activation process α, is the state of the decay and determines the initiation of the mass loss process. 2) Mass loss process, in which irrecoverable mass loss occurs when the α = 1. Increase in the activation process and mass loss occurs when RH ≥ 95% and T > 0 °C. The presented decay modelling was performed using α = 1 as initial state. The presented model output is mass loss (ML) in [%].

2.3.3 Frost damage

The risk of frost damage on the exterior surface was determined using the Delphin output type "moisture saturation degree" (MSD), which is the total moisture volume related to total pore volume. For non-frost resistant materials, the International Association for Science and Technology of Building Maintenance and Monuments Preservation (WTA) recommend that the pore saturation should not exceed 30% (19). The limit of 30% pore saturation is considered as a rather conservative value when dealing with modern masonry bricks, as experimental studies indicate that the critical pore saturation is closer to 80-90% (20) (21). However, frost dilatometry tests by Mensinga et. al. (20) suggests that historical masonry bricks may have a critical pore saturation as low as 25-30%. In addition, the Delphin output type "Ice volume to pore volume ratio" (ICE) (22), was also used for predicting the potential risk of frost damage.

3 Results and discussion

This section presents the measured values of RH, and the damage models derived from the measured temperatures and RH; followed by the simulated RH and associated damage models. The presented data are hourly averages of the logged measurements, and data is presented for the period May 1, 2015 to May 1, 2017. Furthermore, assessment of the measurement data showed that while the thermal conditions in the test walls stabilized within a few months, the moisture conditions stabilized after around 12 months, presumably due to large amounts of building moisture. Data is presented for the entire period, however for this reason focus will be on the 2nd year of the period, and the damage models was first initiated at the beginning of the 2nd year. The results and discussion parts have been combined for easier presentation of the results.

3.1 Field study

The measured RH data is presented for points of interest within the test walls together with the results from the respective damage models. Note that for simplicity of presentation, the measured temperature data will not be presented, although the data is a critical element in understanding the significance of the measured RH. The temperature data was however included in the assessment of the hygrothermal conditions using the damage models.

3.1.1 The interface

The measurements in Figure 3 show condensation at the interface (Point 3) in all the insulated walls during winter. Wall 2 experience near 100% RH with minor fluctuations during summer, while the exterior hydrophobization of Walls 3 and 6 are seen to reduce the RH compared to the un-hydrophobized Wall 2. The measurements do however suggest that the effect of the hydrophobization varies depending on the season; where in summer the RH is decreased as rain penetration is reduced due to the hydrophobization. In winter, the RH increases rapidly as the hydrophobization reduces the liquid transport through the outermost part of the masonry wall. Resulting in a reduced potential for evaporation to the cold outdoor climate during winter. The observed increase in RH caused by the internal insulation and the reduction by the hydrophobization correlate with findings from other studies including (4) (12), assessing the performance through hygrothermal simulations.
For the risk of mould growth, the highest mould index (M) is seen for the un-hydrophobized Wall 2: M = 2.6, while lower mould indexes are seen for the hydrophobized Walls 3 and 6: M = 0.8 and M = 0.9 respectively. The threshold of M < 3 suggested by (17) was not exceeded within the measurement period, however the results are based on one year of data, and all three walls show an increasing trend during the winter period.

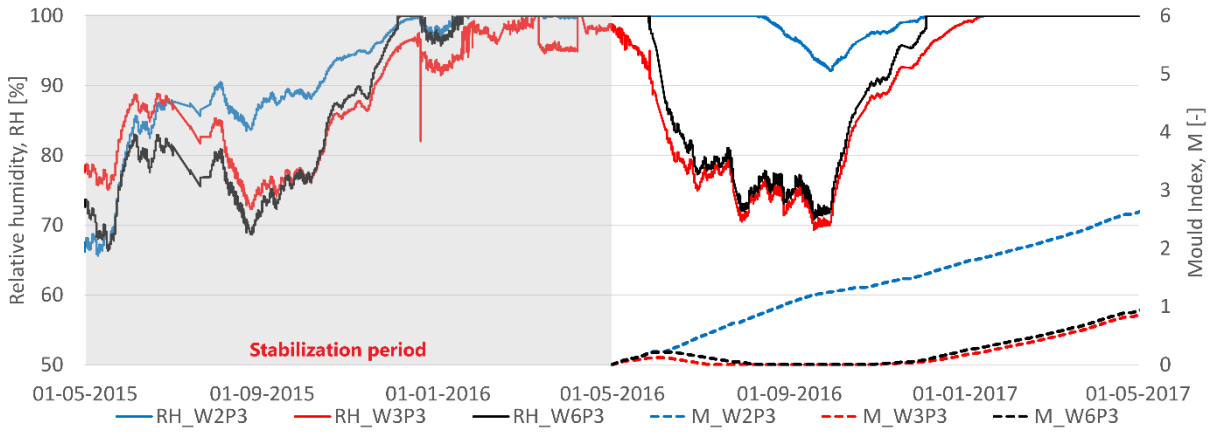

Figure 3 Measured RH and calculated Mould Index, M for the sensor at the interface: Point 3. Source: Tommy Riviere Odgaard and Nickolaj Feldt Jensen

3.1.2 The embedded wooden wall plate

In traditional application of internal insulation, the same system configuration is used for the entire wall surface – from floor to ceiling. Insulation installed in front of the embedded wooden wall plate supporting the floor beams may however pose a problem, as the reduced heat flow decreases the temperature in the wall plate resulting in increased RH. The magnitude of the increase could be so severe that it may result in wood decay in the wall plate. Considering the measurements for the reference Wall 5 and the insulated Wall 2 (Figure 4), the RH and mass loss by decay (ML) is seen to increase due to the application of the internal insulation. From the ML

curves it is also seen that the decay occurs one month earlier in the spring for the insulated Wall 2 compared to the reference Wall 5. Note also that the difference in RH in the wall plate is largest during the winter, when the temperature difference between the indoor and outdoor is greater. Furthermore, the measurements show that the exterior hydrophobization (Wall 3) reduces the RH in the wall plate to levels lower than that of the reference Wall 5, as the masonry wall surrounding the embedded wooden wall plate becomes drier, which also increases the temperature in the masonry and wall plate slightly, in turn lowering the RH. The risk of wood decay in the wall plate was also reduced. Lastly, the increased heat flow induced by the deliberate thermal bridge installed in front of the embedded wooden wall plate (Wall 6) increases the temperature, which in turn reduces the RH in the wall plate even further. The effect of the thermal bridge is largest during winter, due to larger temperature differences. The risk of wood decay also reduces due to the thermal bridge.

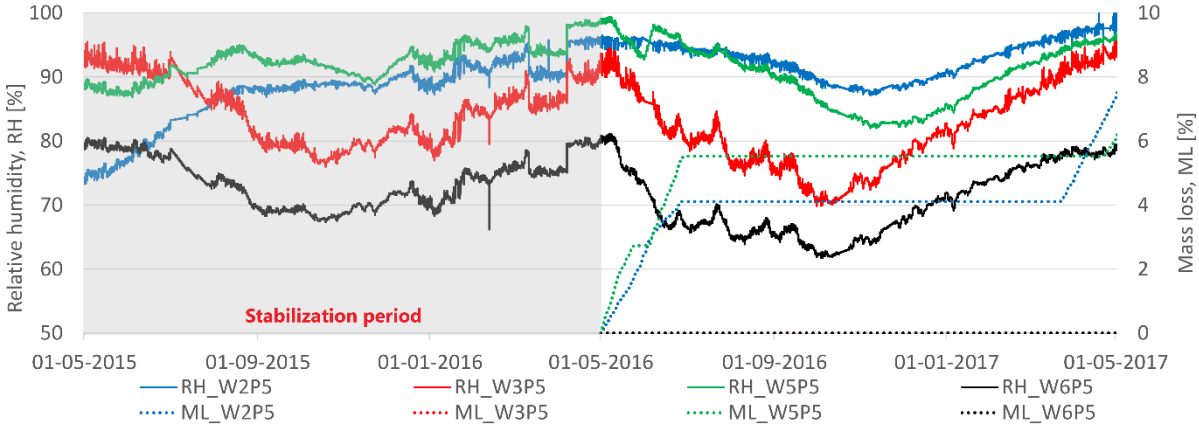

Figure 4 Measured RH and calculated Mass Loss by decay, ML for the sensor in the wooden wall plate: Point 5. Source: Tommy Riviere Odgaard and Nickolaj Feldt Jensen

3.1.3 The embedded wooden beam ends

For the embedded wooden beam ends in Figure 5, rather similar values of RH are seen for the un-hydrophobized reference Wall 5 and the insulated Wall 2. The exterior hydrophobization (Wall3) reduces the RH in the beam end during summer, while in autumn and winter the RH increases to levels above those of the un-hydrophobized walls. Lastly, the deliberate thermal bridge installed in front of the embedded wooden wall plate (Wall 6) reduces the RH even further during summer and reducing the magnitude of the increase in autumn and winter; resulting in RH levels like those seen for the un-hydrophobized walls. The increased RH for the hydrophobized walls seems to be related to the same phenomenon as discussed for the increased RH at the interface.

The hygrothermal conditions for the embedded wooden beam-ends are in general slightly better than seen for the embedded wooden wall plates (Figure 4). Results from the VTT model suggests no wood decay in the beam end for neither the un-hydrophobized Walls 2 and 5 nor the hydrophobized Walls 3 and 6. The presented results are supported by the findings from other studies (3) (23) investigating the performance of solid masonry walls fitted with the internal insulation in combination with deliberate thermal bridge near the floor partition. This indicates worse conditions in the beam ends due to the internal floor-to-ceiling insulation, while a deliberate thermal bridge above or above and below the floor partition reduces the increase in RH caused by the internal insulation.

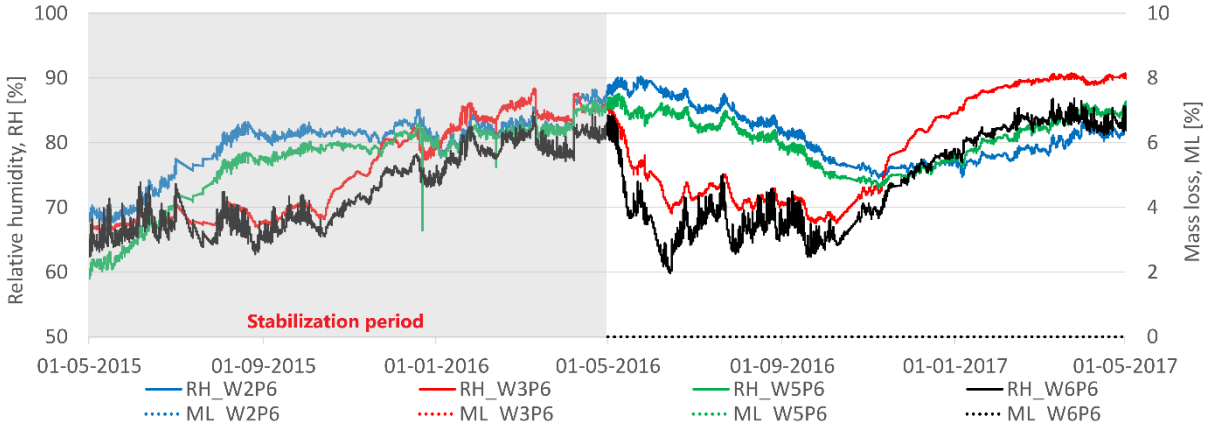

Figure 5 Measured RH and calculated Mass Loss by decay, ML for the sensor in the wooden beam end: Point 6. Source: Tommy Riviere Odgaard and Nickolaj Feldt Jensen

3.1.4 The interior surface

The internally insulated Walls 2, 3 and 6 reduces the RH at the interior surface (Point 4) by 10-15% compared to reference Wall 5 (Point 3) (Figure 6). The un-hydrophobized Wall 2 shows higher RH during summer of 2016 than the hydrophobized Walls 3 and 6, however in the following autumn, winter and spring the three walls show rather similar levels. The RH at the interior surface in front of the deliberate thermal bridge (Wall 6, Point 10) is close to the insulated Walls 2, 3 and 6 (Point 4) during the summer of 2016. Then in winter 2016-17, the RH at the interior surface starts to follow that seen for reference Wall 5 (Point 3). The differences in RH observed at the interior surface is the result of the difference in the added thermal resistance by the insulation, hydrophobization (causing drying of the masonry) and the thermal bridge material respectively, all raising the interior surface temperature resulting in reduced RH. No risk of mould growth is seen for the interior surfaces.

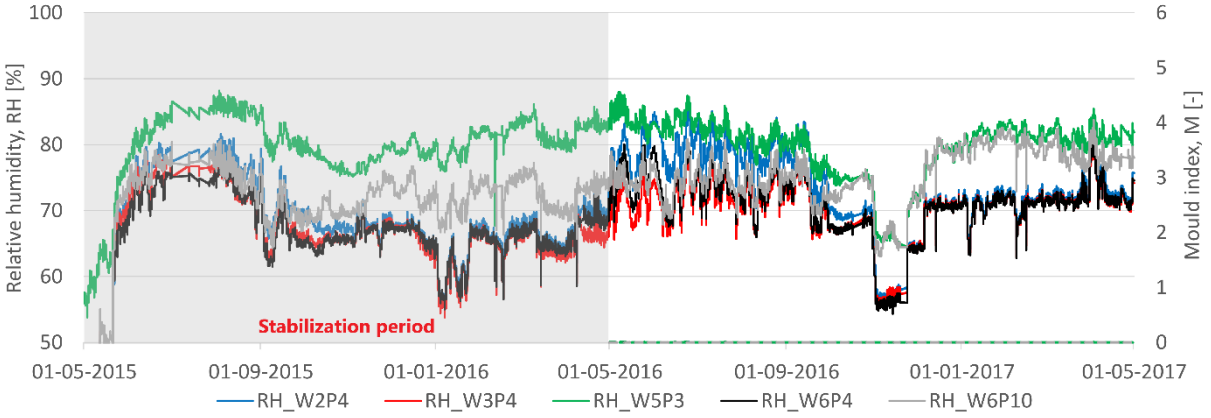

Figure 6 Measured RH and calculated Mould Index, M for the sensor at the interior surface: Points 3,4,10. Source: Tommy Riviere Odgaard and Nickolaj Feldt Jensen

3.2 Simulation study

Results from the field study indicate a need to control the indoor moisture load, for example by mechanical ventilation, to reduce the risk of moisture induced damages. As reference Wall 5 subjected to an indoor RH of 60% (the upper limit for residential buildings) showed risk of wood decay in the embedded wooden wall plate prior to application of the internal insulation (Figure 4), suggesting that the test wall may already have problems with moisture. Furthermore, Walls 2 in Figure 3 and Figure 4 show unacceptable conditions for the internally insulated masonry wall, suitable for mould growth and wood decay. 1-D hygrothermal simulations were therefore carried out with reduced indoor RH.

Results are presented for the un-hydrophobized Wall 2 and the hydrophobized Wall 3 simulated with 60 and 40% indoor RH, together with results from the respective damage models.

3.2.1 The interface

For the interface (Figure 7), the reduction of the indoor RH for the un-hydrophobized Wall 2 shows little to no difference in winter, where both walls show levels near 100% RH. However, in summer the lower indoor RH greatly reduces the levels at the interface. For the hydrophobized Wall 3, the lower indoor RH decreases the levels at the interface throughout the simulation period, with around 20% during summer and 10% during winter. For the calculated risk of mould growth, Wall 2 with 60% indoor RH peaks at M = 1.5, while Wall 2 with 40% indoor RH and the two Wall 3 cases maintains M < 0.5. Note that like the risk of mould calculated from the experimental measurements, the un-hydrophobized Wall 2 with 60% indoor RH shows an increasing trend throughout the period; while the three other cases show slight increase in winter followed by decrease in summer.

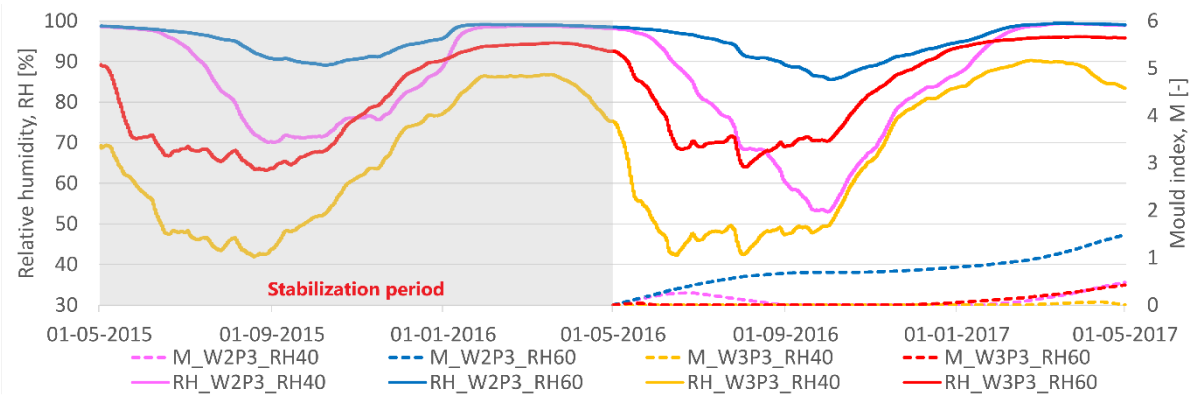

Figure 7 Simulated RH and Mould Index, M for the interface: Point 3. Source: Nickolaj Feldt Jensen

3.2.2 The interior surface

The simulation results for the interior surface will not be presented visually in this paper. As seen for the calculated risk of mould growth based on the experimental measurements, the VTT model did not show a risk of mould growth on the interior surfaces. Lowered indoor RH reduced the levels at the interior surface throughout the simulated period for all the wall models.

3.2.3 The exterior surface

The reduction of the indoor RH did not affect the results at the exterior surface greatly with respect to the risk of frost damage, as MSD and ICE were almost identical for the simulated models with 60 and 40%. Therefore, results are only presented for the wall models simulated with 60% RH. In Figure 8 it is seen that with the exception of one event occurring in July 2015, neither the MSD or ICE ratios exceed the critical threshold of 30% by WTA (19), suggesting that frost damage will not occur in the test walls. This correlates with the visual inspections of the test walls which did not show any signs of frost induced damage.

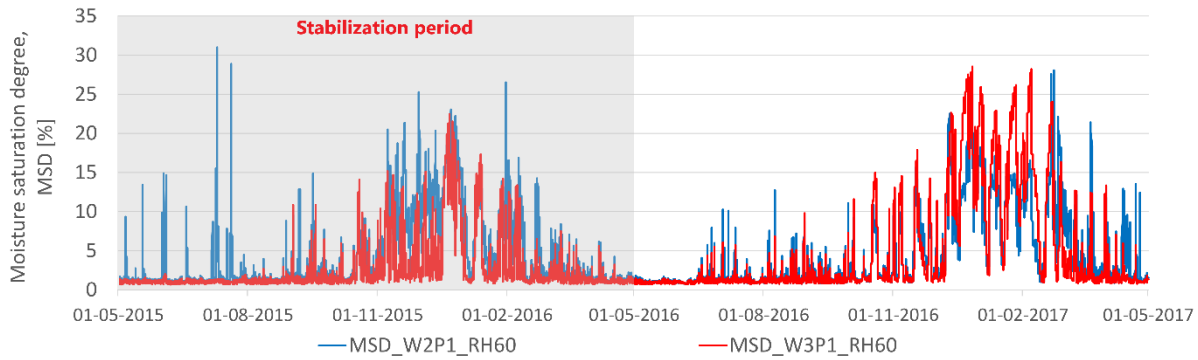

Figure 8 Simulated MSD for the exterior surface: Point 1. Source: Nickolaj Feldt Jensen

Comparison between the un-hydrophobized Wall 2 and the hydrophobized Wall 3 with respect to MSD (Figure 8) shows large increase during the summer of 2015 for Wall 2, which is not seen for Wall 3. This suggests that reduced rain intrusion by the hydrophobization causes the low MSD. Similar is seen during winter 2015-16, where the two walls are rather similar with the exceptions of several peaks in Wall 2. A different situation is however seen during winter 2016-17, where Wall 3 experiences several peaks in MSD, which are not seen in Wall 2. This is also seen in Figure 9 showing the pore ice volume ratio; in which the period December 1, 2016 to May 1, 2017 is emphasized. On several occasions during this period, ICE in Wall 3 is seen to be around twice of what is seen in Wall 2. These results may be related to the issue of the hydrophobization limiting the liquid transport through the outermost part of the masonry wall, resulting in an increased moisture levels.

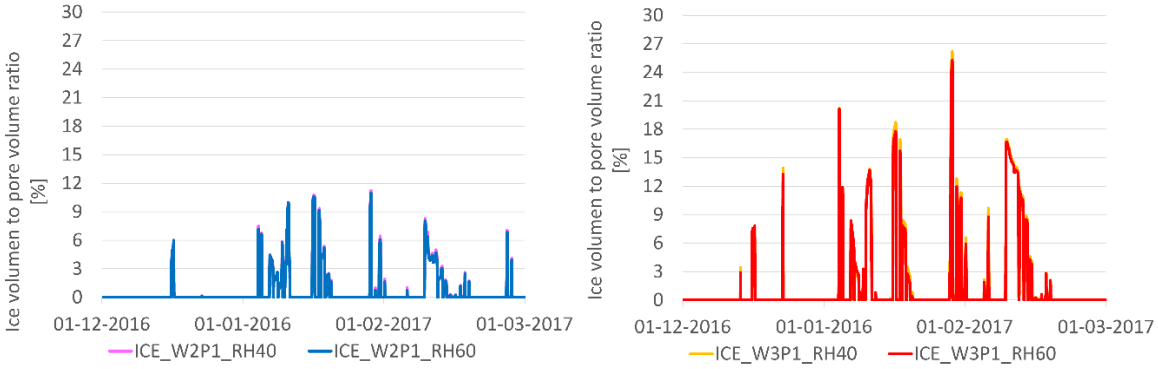

Figure 9 Simulated ICE at the exterior surface: Point 1. Source: Nickolaj Feldt Jensen

4 Conclusion

Measurements from several solid masonry walls fitted with diffusion-open, capillary active insulation based on lightweight autoclaved aerated concrete, indicate that internal post insulation of these walls exacerbate the hygrothermal conditions at the interface between the existing wall and the insulation system. This increases the risk of mould growth at the interface. Furthermore, exterior hydrophobization has both positive and negative effects on the hygrothermal conditions of the wall. A reduction of the rain intrusion in summer reduces the RH in the wall. During winter, the reduced liquid transport from the inside is inhibited by the hydrophobization, and thus limits the evaporation to the cold dry outdoor climate. This is seen both at the interface and in the wooden beam ends. In addition, installation of a deliberate thermal bridge in front of the embedded wooden wall plate has a positive influence on the hygrothermal conditions in wall plate by reducing the RH and the risk of wood decay. In the beam ends, the deliberate thermal bridge reduces the increase in RH caused by the exterior hydrophobization, resulting in levels close to the un-hydrophobized walls. Conditions in the wooden beam end are less critical and no wood decay is predicted. Finally, the simulation study investigating the effect of reduced indoor RH for internally insulated solid masonry walls with and without hydrophobization indicates that a reduction of the indoor RH to 40% (for example by mechanical ventilation) decreases the risk of mould growth at the interface during the whole year. If the RH is reduced only during winter time, then this will also decrease the risk of mould growth.

5 Acknowledgements

Xella Denmark is acknowledged for supply and installation of the Ytong Multipor insulation system, and Intro Flex Aps for supply and application of Remmers Funcosil FC hydrophobization for the exterior surfaces. The work was planned in collaboration with Xella Denmark and the work was financially supported by Realdania, which is gratefully acknowledged. None of the project partners have had any influence on the results presented in this paper.

References

1. *Interior Insulation—Characterisation of the Historic, Solid Masonrybuilding Segment and Analysis of the Heat Saving Potential by 1d, 2d,and 3d Simulation.* **Odgaard, Tommy Riviere, Bjarløv, Søren Peter and Rode, Carsten.** s.l. : ELSEVIER SCIENCE SA, 2018, Energy and Buildings, Vol. 160, pp. 1-11.

2. *Hygrothermal performance of internally insulated brick wall in cold climate: A case study in a historical school*

building. **Klõšeiko, Paul, Arumaegi, Endrik and Kalamees, Targo.** 5, s.l. : SAGE PUBLICATIONS LTD, 2015, J. Build. Phys., Vol. 38, pp. 444-464.

3. *Investigation of interior post-insulated masonry walls with wooden beam ends.* **Morelli, Martin and Svendsen, Svend.** 2012, J. Build. Phys., Vol. 36, pp. 265-293.

4. *Effect of façade impregnation on feasibility of capillary active thermal internal insulation for a historic dormitory – A hygrothermal simulation study.* **Finken, Gholam R., Bjarløv, Søren P. and Peuhkuri, Ruut H.** s.l. : ELSEVIER SCI LTD, 2016, Construction and Building Materials, Vol. 113, pp. 202-214.

5. *Full-Scale Test of an Old Heritage Multi-Storey Building Undergoing Energy Retrofitting with Focus on Internal Insulation and Moisture.* **Harrestrup, Maria and Svendsen, Svend.** s.l. : PERGAMON-ELSEVIER SCIENCE LTD, 2015, Building and Environment, Vol. 85, pp. 123-133.

6. *Effect of interior and exterior insulation on the hygrothermal behaviour of exposed walls.* **Künzel, Hartwig M.** s.l. : SPRINGER, 1998, Materials and Structures, Vol. 31, pp. 99-103.

7. *Interior insulation retrofits of load-bearing masonry walls in cold climates.* **Straube, John and Schumacher, Chris.** 2, 2007, Journal of Green Building, Vol. 2, pp. 42-50.

8. **Brandt, Erik, et al.** *SBi-Anvisning 224 - Fugt i Bygninger 2nd Edition (Danish).* Hørsholm, Denmark : Statens Byggeforskningensinstitut, Aalborg University, 2013.

9. **Christensen, Georg, Koch, Anne Pia and Møller, Eva B.** *Erfaringsblad (31) 15 11 15: Indvendig efterisolering - ældre ydervægge af murværk (Danish).* Copenhagen, Denmark : BYG-ERFA, 2015.

10. *DS/EN ISO 13788:2012 Hygrothermal performance of building components and building elements - Internal surface temperature to avoid critical surface humidity and interstitial condensation - Calculation methods, 2. edition.* Charlottenlund, Denmark. : Dansk Standard/Danish Standards, 2013.

11. **Hansen, Ernst Jan de Place, et al.** *SBi-Anvisning 230 - Anvisning om Bygningsreglement 2010 (in Danish).* Hørsholm, Denmark : Statens Byggeforskningsinstitut, Aalborg University, 2010.

12. **Otiv, Peter.** *Hygrothermal modelling of internal insulation to solid masonry walls.* s.l. : N.p., 2016. MSc. Thesis, Technical University of Denmark, Kgs. Lyngby, Denmark.

13. **Dysted, Daniel and Sandholdt, Hasse.** *Experimental and theoretical investigation of Interior insulation of solid brick walls with foam concrete and another silicate based material.* Kgs. Lyngby, Denmark : Technical University of Denmark, 2015.

14. **Häkkinen, Tarja, et al.** *SUSREF: Sustainable refurbishment of exterior walls and buildnig facades. Final report Part A – Methods and recommendations.* Espoo, Finland : VTT Technical Research Centre of Finland, 2012.

15. *A mathematical model of mould growth on wooden material.* **Hukka, A. and Viitanen, H. A. .** 6, 1999, Wood Science and Technology, Vol. 33, pp. 475-485.

16. *Mold Growth Modeling of Building Structures Using Sensitivity Classes of Materials.* **Ojanen, Tuomo, et al.** 2010. Thermal Performance of the Exterior Envelopes of Buildings XI. pp. 1-10.

17. *Mold Risk Classification Based on Comparative Evaluation of Two Established Growth Models.* **Viitanen, H., et al.** Torino, Italy : s.n., 2015. 6th International Building Physics Conference, IBPC 2015.

18. *Towards modelling of decay risk of wooden materials.* **Viitanen, H., et al.** 2010, European Journal of Wood and Wood Products,, pp. 303-313.

19. **WTA.** *Interior insulation according to WTA II, Instruction Sheet 6-5.* Pfaffenhofen, Germany : WTA (Wissenschaftlich-Technische Arbeitsgemeinschaft für Bauwerkserhaltung und Denkmalpflege), 2014.

20. *Assessing the freeze-thaw resistance of clay brick for interior insulation retrofit projects.* **Mensinga, Peter, Straube, John and Schumacher, Christopher.** Clearwater Beach, Florida, USA : American Society of Heating, Refrigeration, and Air-Conditioning Engineers (ASHRAE), 2010. 11th International Conference on Thermal Performance of the Exterior Envelopes of Whole Buildings, Buildings XI.

21. *Towards a limit states approach to insulating solid masonry walls in a cold climate.* **Rose, D. De, et al.** Toronto, Canada : NBEC Cananda, 2014. 14th Canadian Conference on Building Science and Technology.

22. *Implementation of an efficient numerical solution method to simulate freezing processes in porous media.* **Nicolai, Andreas and Sontag, Luisa. Vienna,** Austria : s.n., 2013. Central European Symposium on Building Physics.

23. *Internal insulation applied in heritage multi-storey buildings with wooden beams embedded in solid masonry brick façades.* **Harrestrup, Maria and Svendsen, Svend.** 2016, Building and Environment, Vol. 99, pp. 59-72.

Authors

Nickolaj Feldt Jensen
Technical University of Denmark
Department of Civil Engineering
Brovej 118
2800 Kgs. Lyngby, Denmark
nicf@byg.dtu.dk

Søren Peter Bjarløv
Technical University of Denmark
Department of Civil Engineering
Brovej 118
2800 Kgs. Lyngby, Denmark
spb@byg.dtu.dk

Carsten Rode
Technical University of Denmark
Department of Civil Engineering
Nils Koppels Allé 402
2800 Kgs. Lyngby, Denmark
car@byg.dtu.dk

Tommy Riviere Odgaard
COWI A/S
Section of Building Physics and Refurbishment
Parallelvej 2
2800 Kgs. Lyngby, Denmark
TOOG@COWI.com